Open access • Journal Article • DOI:10.1193/030113EQS060M

Ground Motion and Seismic Source Aspects of the Canterbury Earthquake Sequence — Source link

Brendon Bradley, Mark Quigley, Russ Van Dissen, Nicola Litchfield

Institutions: University of Canterbury, GNS Science

Published on: 01 Feb 2014 - Earthquake Spectra (Earthquake Engineering Research Institute)

Topics: Peak ground acceleration, Earthquake simulation, Seismic hazard and Seismic microzonation

Ground Motion and Seismic Source Aspects of the Canterbury Earthquake Sequence

Brendon A. Bradley,[a)] M.EERI, Mark C. Quigley,[a)] Russ J. Van Dissen,[b)] and Nicola J. Litchfield[b)]

This paper provides an overview of the ground motion and seismic source aspects of the Canterbury earthquake sequence. Common reported attributes among the largest earthquakes in this sequence are complex ruptures, large displacements per unit fault length, and high stress drops. The Darfield earthquake produced an approximately 30 km surface rupture in the Canterbury Plains with dextral surface displacements of several meters, and a subordinate amount of vertical displacement, impacting residential structures, agricultural land, and river channels. The dense set of strong ground motions recorded in the near-source region of all the major events in the sequence provides significant insight into the spatial variability in ground motion characteristics, as well as the significance of directivity, basin-generated surface waves, and nonlinear local site effects. The ground motion amplitudes in the 22 February 2011 earthquake, in particular, produced horizontal ground motion amplitudes in the Central Business District (CBD) well above those specified for the design of conventional structures. [DOI: 10.1193/030113EQS060M]

INTRODUCTION

The 2010–2011 Canterbury earthquake sequence includes the 4 September 2010 M_w7.1 Darfield earthquake (e.g., Gledhill et al. 2011) and three subsequent earthquakes of $M_w \geq 5.9$, most notably the 22 February 2011 M_w6.2 Christchurch earthquake (e.g., Kaiser et al. 2012) that resulted in 185 fatalities. All of the earthquakes occurred on previously unknown faults. The Darfield earthquake was the only event in which a surface rupture was generated (Figure 1a), causing significant damage to houses (Figure 1c), roads, power poles, and agricultural land, among others (Quigley et al. 2012, Van Dissen et al. 2011). Ground shaking in the Darfield earthquake resulted in widespread liquefaction in eastern Christchurch and in isolated areas throughout the region (Cubrinovski et al. 2010) and substantial damage to unreinforced masonry structures (Dizhur et al. 2010).

The M_w6.2 Christchurch earthquake caused significant damage to commercial and residential buildings of various eras (Buchanan et al. 2011, Clifton et al. 2011, Kam et al. 2011). The severity and spatial extent of liquefaction observed in native soils was profound and was the dominant cause of damage to residential houses, bridges, and underground lifelines

[a)] University of Canterbury, Private Bag 4800, Ilam, Christchurch, New Zealand
[b)] GNS Science, P.O. Box 30368, Lower Hutt, Wellington, New Zealand

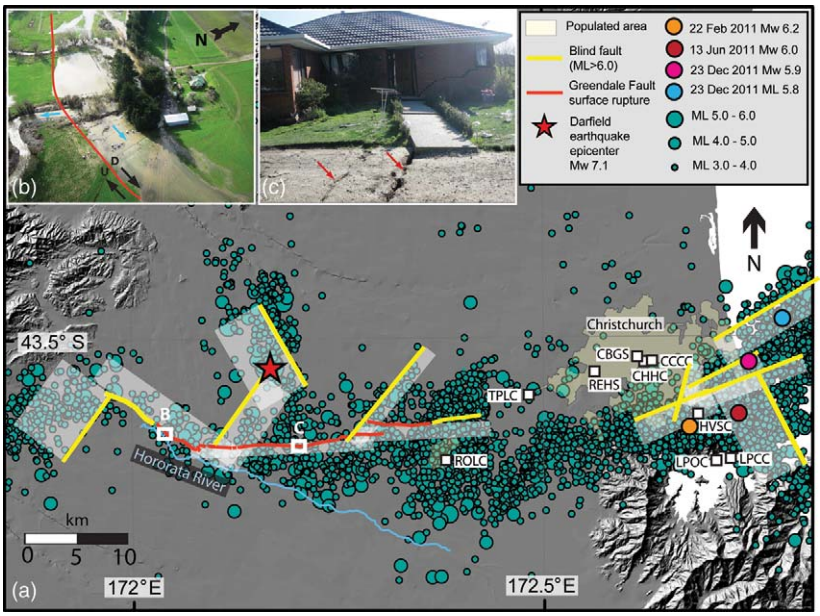

Figure 1. (a) Epicenter locations for $M_L \geq 3.0$ events from 4 September 2010 to 10 February 2013 (data from www.geonet.org.nz). Projected surface locations of major blind faults in yellow and subsurface locations in transparent white (from Beavan et al. 2012) and location of mapped surface ruptures in red (from Quigley et al. 2012). Locations of selected strong ground motion stations as shown; full station names appear in Table 1. (b) Partial avulsion and related flooding of the Hororata River in the Darfield earthquake. Mapped Greendale fault trace from Duffy et al. (2013) in red; black arrows and "U" (up) and "D" (down) denote relative movement across fault. Blue arrows denote river flow direction. (c) Greendale fault traces running through residential property. Note lack of dwelling collapse despite being situated directly on the surface fault rupture.

(Cubrinovski et al. 2011a). Rockfall and cliff collapse occurred in many parts of southern Christchurch (Massey et al. 2014, Dellow et al. 2011). The 13 June 2011 M_w6.0 earthquake caused further damage to previously damaged structures and severe liquefaction and rockfalls, and similarly for the M_w5.8 and M_w5.9 earthquakes on 23 December 2011. Several additional smaller aftershocks have also induced localized surface manifestations of liquefaction (e.g., Quigley et al. 2013), rockfall, and building damage. This paper provides a summary of seismic sources and ground motion characteristics of the Canterbury earthquake sequence in order to provide context for subsequent papers in this special issue on structural, geotechnical, and lifeline performance.

CHARACTERISTICS OF SEISMIC SOURCES

The Canterbury sequence occurred within ~30 km thick continental crust in a relatively low strain rate region at the periphery of the Pacific–Australian plate boundary deformation zone in New Zealand's South Island. The local geology consists of Mesozoic greywacke

bedrock variably overlain by a 1–2 km thick package of Late Cretaceous to Neogene sedimentary and volcanic rocks and Pliocene to Quaternary alluvial gravels that locally exceed 1 km in thickness. GPS-derived principal horizontal contraction in the region occurs at 16 nanostrain/year with an azimuth of 110–120° (Wallace et al. 2007).

The 4 September 2010 M_w7.1 Darfield earthquake was a complex event, beginning on a steep reverse fault and involving the rupture of at least 7 fault segments including EW-striking right-lateral faults, NE-striking reverse faults, NNW-striking left-lateral faults, and NW-striking normal right-lateral faults (Beavan et al. 2012, Elliott et al. 2012). The largest moment release resulted from the right-lateral rupture of the Greendale fault (equivalent to a $M_w6.9-7.0$ earthquake), which was the only fault to generate a surface rupture (Figure 1a). Maximum subsurface slip was concentrated at depths of 2–6 km (Beavan et al. 2012) and may have exceeded 7 m over a strike length of ~7 − 8 km (Elliott et al. 2012). The combined subsurface fault length is inferred to be ~48 km (Beavan et al. 2012). The inferred rupture extents of other blind faults (Figure 1a) that ruptured in the Darfield earthquake range from 0.5–1 km depth (Beavan et al. 2012), suggesting that rupture likely ceased near the base of the Pliocene (~1 km) or Quaternary (~0.5 km) sedimentary deposits (Jongens et al. 2012). The 29.5 ± 0.5 km–long Greendale fault surface rupture had a maximum surface displacement of 5.3 m (Quigley et al. 2012). Surface displacement measurements in the central Greendale fault above areas of maximum inferred subsurface slip typically range from 4–5 m (Figure 2), indicating an apparent decrease in coseismic slip toward the surface. Steps in the fault surface slip gradients occur in fault trace step-overs and where other blind faults project to intersect the Greendale fault (Figures 1 and 2).

The 22 February 2011 M_w6.2 Christchurch earthquake involved the rupture of 2–3 blind faults (Figure 1a) with reverse and right-lateral displacements (Beavan et al. 2012). Inferred rupture extents were ~0.5 km depth below surface, suggesting rupture termination in Miocene volcanic rocks. Maximum coseismic slip was 2.5–3 m at depths of 4–6 km (Beavan et al. 2012, Elliott et al. 2012). The 13 June 2011 M_w6.0 earthquake likely involved an intersecting ENE-striking reverse-right lateral fault and NW-striking left-lateral fault with ~1 km–deep rupture extent and maximum subsurface slip of <1 m (Beavan et al. 2012). The 23 December 2011 M_w5.8 and M_w5.9 earthquakes ruptured 1–2 largely offshore, NE-striking reverse-right-lateral, blind faults with maximum slip of >1.4 m occurring at depths of 2–5 km and rupture extents of ~1 km deep (Beavan et al. 2012).

Large surface-slip-to-surface-rupture length was reported for the Greendale fault by Quigley et al. (2012), and large subsurface-slip-to-subsurface-fault length ratios were reported for the Christchurch earthquake source (Beavan et al. 2012, Elliott et al. 2012), implying that large slip-per-unit fault length may be a characteristic of some of the faults in this region. Using surface rupture data and an elliptical fault displacement model, Quigley et al. (2012) computed a static stress drop of 13.9 ± 3.7 MPa for the Greendale fault rupture in the Darfield earthquake. Using InSAR-derived fault models, Elliot et al. (2012) computed stress drops of 6–11 MPa for individual fault segments in the Darfield earthquake and 14 MPa for the Christchurch earthquake. These results are consistent with reported stress drops from earthquakes on other faults with long recurrence intervals near the periphery

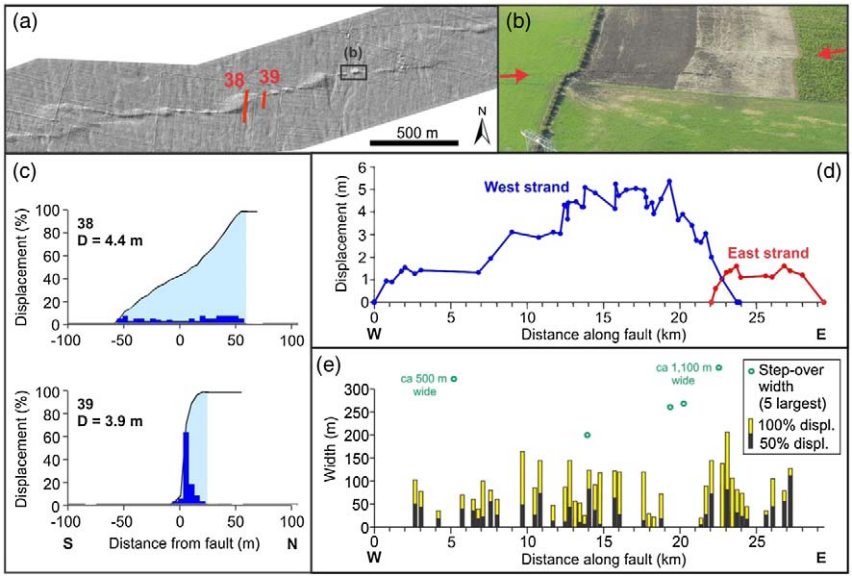

Figure 2. (a) LiDAR hillshade image of a typical section of the Greendale fault surface rupture. (b) Photo showing along-strike variation of surface rupture deformation zone width (the two bare fields are each ~40 m wide, and total right-lateral displacement is ~4.5 m). (c) Plots of cumulative strike-slip surface rupture displacement and histograms of displacement distribution at two representative sites across the Greendale fault, illustrating that surface rupture deformation is widest, and more evenly distributed, at step-overs (profile 38), and narrowest and more spiked where rupture comprises a single trace (profile 39). (d) Net surface rupture displacement along the Greendale fault (after Quigley et al. 2012). (e) Width (horizontal distance) measured perpendicular to fault strike over which it takes to accumulate 50% and 100% of the total dextral surface rupture displacement at 40 sites along the Greendale fault (after Van Dissen et al. 2011).

of plate boundary deformation zones (e.g., 7–12 MPa in Landers-Hector Mine earthquake sequence; Price and Bürgmann 2002). For comparison, Fry and Gerstenberger (2011) calculate the apparent stress of the Darfield and Christchurch earthquakes to be ~16 MPa and ~4 MPa, respectively.

GREENDALE FAULT SURFACE RUPTURE AND ENGINEERING AND LAND-USE IMPLICATIONS

Field mapping and surveying, combined with LiDAR data, was used to define the Greendale fault surface rupture trace (Figure 2). The maximum right-lateral surface displacement was 5.3 m. Vertical displacement was typically on the order of tens of centimeters in flexure and bulging, but at several fault bends, vertical displacement reached 1–1.5 m. Perpendicular to fault strike, surface rupture displacement was distributed across a ~30 m to 300 m wide deformation zone, largely as horizontal flexure (Figures 2c and 2e). On average, 50% of the horizontal displacement occurred over 40% of the total width of the deformation zone, with offset on observable discrete shears, where present, typically accounting

for less than about a third of the total displacement. Characterisations of fault displacement, such as those depicted in Figure 2c, are relevant for both planning fault avoidance set-back distances (e.g., Villamor et al. 2012) and for designing surface rupture–resilient buildings and infrastructure (Bray and Kelson 2006, Rockwell et al. 2002).

About a dozen buildings, mainly single-story houses and farm sheds, were affected by surface rupture, but none collapsed. This was largely because most of the buildings were relatively flexible, resilient timber-framed structures, and also because deformation was distributed over a relatively wide zone. There were, however, notable differences in the respective performances of the buildings. Houses with only lightly reinforced concrete slab foundations suffered moderate to severe structural and nonstructural damage. Three other types of buildings performed more favorably and far exceeded life-safety objectives: one had a robust concrete slab foundation that was stronger than the surrounding soil, another had a shallow-seated pile foundation that isolated ground deformation from the superstructure, and the third had a structural system that enabled the building to tilt and rotate as a rigid body. This third building suffered very little internal deformation, was straightforward to relevel, and demonstrated, serendipitously, the potential for a high degree of post-event functionality for certain types of buildings in relation to, in this case, distributed surface fault rupture (Van Dissen et al. 2011).

In 2003, the Ministry for the Environment (MfE), New Zealand, published best practice guidelines for mitigating surface fault rupture hazard (Kerr et al. 2003, Van Dissen et al. 2006). A key rupture hazard parameter in the MfE guidelines is fault complexity. For a given displacement, the amount of deformation at a specific locality is less within a distributed rupture zone, than it is within a narrow zone. Surface rupture displacement on the Greendale fault was typically distributed across a relatively wide zone of deformation. Buildings located within this distributed zone of deformation were subjected to only a portion of the fault's total surface rupture displacement, and no building within this zone collapsed. This provides a clear example of the appropriateness of the MfE's distributed fault complexity parameter, at least for Building Importance Category 2a buildings (i.e., residential structures) and with respect to life-safety.

CHARACTERISTICS OF EARTHQUAKE-INDUCED GROUND MOTIONS

Table 1 provides a summary of the near-source ground motions resulting from the major events of 4 September 2010, 22 February 2011, 13 June 2011, and 23 December 2011. The largest ground motions in central Christchurch occurred during the 22 February 2011 Christchurch earthquake primarily as a result of its close proximity to the earthquake source. Severe ground motions were observed at numerous strong motion stations over the multiple events. Peak accelerations of up to 1.41 g and 2.21 g were recorded at HVSC in the horizontal and vertical directions, respectively. In the CBD (i.e., CBGS, CHHC, CCCC, and REHS stations), PGA values ranging from 0.37–0.52 g were observed in the 22 February 2011 event.

GROUND MOTION INTENSITY IN THE CENTRAL BUSINESS DISTRICT (CBD)

Figure 3 illustrates the pseudo-acceleration response spectra of four strong motion stations (CCCC, CHHC, CBGS, REHS) located in the CBD region during the aforementioned four events. Despite their geographic separation distances (relative to their respective

Table 1. Strong motion station recordings in Christchurch from the four major Canterbury earthquakes

			4 September 2010 M_w7.1[5]			22 February 2011 M_w6.2[5]			13 June 2011 M_w6.0[5]			23 December 2011 M_w5.9[5]		
Station name	Code	Site class[1]	R_{rup}[2] (km)	PGA[3] (g)	PGV[4] (cm/s)	R_{rup}[2] (km)	PGA[3] (g)	PGV[4] (cm/s)	R_{rup}[2] (km)	PGA[3] (g)	PGV[4] (cm/s)	R_{rup}[2] (km)	PGA[3] (g)	PGV[4] (cm/s)
Canterbury Aeroclub	CACS	D	11.7	0.20	39.2	12.8	0.21	20.0	16.2	0.14	9.7	16.7	0.08	9.8
Christchurch Botanic Gardens	CBGS	D	14.4	0.16	36.2	4.7	0.50	46.3	7.6	0.16	26.0	10.2	0.21	22.4
Christchurch Cathedral College	CCCC	D	16.2	0.22	53.8	2.8	0.43	56.3	–	–	–	8.7	0.18	22.3
Christchurch Hospital	CHHC	D	14.7	0.17	38.3	3.8	0.37	50.9	6.8	0.22	31.6	10.0	0.22	21.0
Cashmere High School	CMHS	D	14.0	0.24	31.3	1.4	0.37	44.4	7.1	0.18	28.4	12.0	0.17	19.2
Hulverstone Dr Pumping Station	HPSC	E	21.7	0.15	39.3	3.9	0.22	36.7	5.5	0.26	34.7	3.2	0.26	41.5
Heathcote Valley School	HVSC	C	20.8	0.61	28.8	4.0	1.41	81.4	3.6	0.91	55.3	9.7	0.44	22.3
Kaipoi North School	KPOC	E	27.6	0.34	35.7	17.4	0.20	18.9	19.4	0.10	11.2	–	–	–
Lincon School	LINC	D	5.9	0.44	74.4	13.6	0.12	12.7	21.0	0.06	12.1	25.9	0.07	6.5
Lyttelton Port	LPCC	B	22.1	0.29	19.1	7.1	0.92	45.6	5.8	0.64	32.6	12.4	0.44	22.8
New Brighton Library	NBLC	D	–	–	–	–	–	–	4.1	0.21	36.8	–	–	–
North New Brighton School	NNBS	E	23.1	0.21	35.6	3.8	0.67	35.1	5.6	0.20	31.8	–	–	–
Papanui High School	PPHS	D	15.3	0.22	54.8	8.6	0.21	36.7	10.4	0.12	19.3	10.5	0.14	18.6
Pages Rd Pumping Station	PRPC	E	19.3	0.21	44.9	2.5	0.63	72.8	3.7	0.34	60.3	–	–	–
Christchurch Resthaven	REHS	D	15.8	0.25	42.6	4.7	0.52	65.4	6.8	0.26	42.5	8.8	0.25	43.8
Riccarton High School	RHSC	D	10.0	0.21	39.3	6.5	0.28	29.8	11.8	0.19	17.6	14.6	0.16	16.9
Rolleston School	ROLC	D	2.2	0.34	73.7	19.6	0.18	8.4	26.8	0.05	5.7	30.6	0.06	3.6

Shirley Library	SHLC	D	18.6	0.18	43.0	5.1	0.33	67.8	6.3	0.18	34.5	6.1	0.28	24.0
Styx Mill Transfer Station	SMTC	D	17.5	0.18	36.1	10.8	0.16	27.6	12.0	0.08	13.0	10.4	0.15	13.0
Templeton School	TPLC	D	3.0	0.27	55.6	12.5	0.11	11.3	19.1	0.06	7.8	22.2	0.08	5.2

[1] As defined by the New Zealand Loadings Standard, NZS1170.5 (2004), that is, B = rock, C = shallow soil, D = deep or soft soil, and E = very soft soil.
[2] Closest distance from fault plane to site based on Beavan et al. (2010, 2011, 2012).
[3] Peak ground acceleration.
[4] Peak ground velocity.
[5] Moment magnitudes from GeoNet (http://www.geonet.org.nz/), the corresponding USGS estimates for these events are: 7.0, 6.1, 5.9, 5.9 (http://earthquake.usgs.gov/earthquakes/). Ground motion parameters are geometric mean horizontal definition.

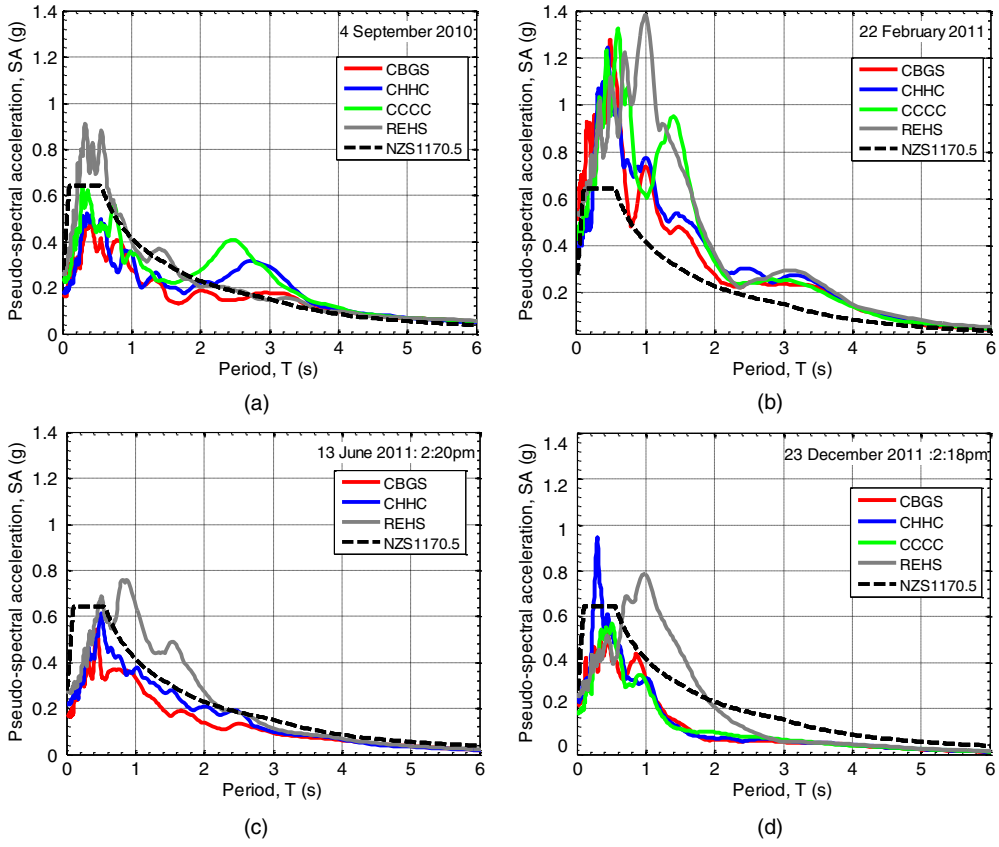

Figure 3. Geometric mean pseudo-spectral acceleration observed in the Christchurch CBD during the: (a) 4 September 2010, M_w7.1; (b) 22 February 2011, M_w6.2; (c) 13 June 2011, M_w6.0; (d) 23 December 2011, M_w5.9 Canterbury earthquakes. No recording at CCCC was obtained in the 13 June 2011 event.

source-to-site distances), the characteristics of the ground motion observed at these locations are relatively similar. This is particularly the case for long-period ground motion ($T > 3$ s) amplitudes, which have longer wavelengths and therefore are expected to be more coherent. On the other hand, at short vibration periods there is a more pronounced difference in accelerations due to the ability of shorter wavelength energy to sample local heterogeneities in the crust, including the local nonlinear response of significantly different surficial soil layers (Cubrinovski et al. 2011b). During the 4 September 2010 Darfield earthquake, with the exception of Resthaven (REHS), ground motion amplitudes were generally below the design spectra for short-to-moderate periods (i.e., $T < 2$ s), and greater at $T = 2-3$ seconds. For the 22 February 2011 Christchurch earthquake, ground motion amplitudes were greater than the 500-year design spectra at all vibration periods. The 13 June 2011 M_w6.0 event produced ground motions nearly equal to design spectral ordinates over a wide range of periods, while the 23 December 2011 M_w5.9 event produced

significant spectral amplitudes primarily only at short-to-moderate vibration periods (with the exception of the REHS station).

NEAR-SOURCE FORWARD DIRECTIVITY EFFECTS

Forward directivity effects were particularly significant for the 4 September 2010 Darfield earthquake as a result of its magnitude (M_w7.1), strike-slip faulting mechanism, and rupture propagation of the central and eastern section of the Greendale fault toward Christchurch (Bradley 2012a). In contrast, forward directivity effects from the 22 February 2011, 13 June 2011, and 23 December 2011 earthquakes were more spatially focused relative to the Darfield earthquake, as a result of their sizes (M_w6.2, 6.0, and 5.9) and shorter rupture durations.

Figure 4 illustrates, as examples, the observed velocity time series at Templeton (TPLC) and Rolleston (ROLC) during the 4 September 2010 Darfield earthquake in which forward directivity effects are clearly evident. At ROLC, the peak ground velocity (PGV) exceeds 100 cm/s in the fault normal direction, as compared to approximately 60 cm/s in the fault parallel direction, while at TPLC, PGVs are approximately 80 cm/s and 30 cm/s in the fault normal and parallel orientations, respectively.

SEDIMENTARY BASIN–GENERATED SURFACE WAVE EFFECTS

Christchurch is located on a sedimentary fan deposit, inter-fingered with estuarine deposits and the volcanic rock of Banks peninsula located to the southeast (Brown and Weeber 1992). Significant long period ground motion was observed at numerous sites, in particular in the 4 September 2010 and 22 February 2011 earthquakes, resulting from basin-induced surface waves (Bradley 2012c, Bradley and Cubrinovski 2011), in addition to the large-amplitude, long-period ground motion resulting from forward directivity associated with source rupture effects. Figure 4a, for example, suggests that the velocity pulse associated with forward directivity at TPLC was subsequently followed by several cycles of

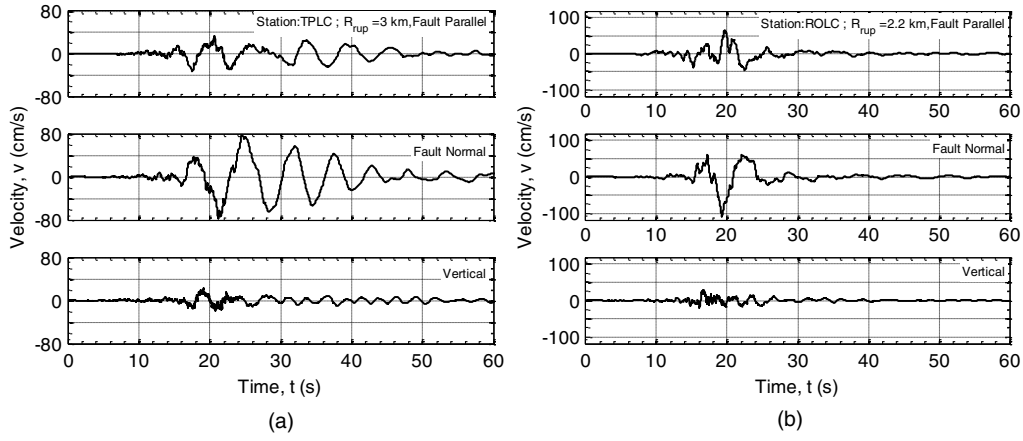

Figure 4. Evidence of strong forward directivity effects at locations to the east of the Greendale fault: (a) Templeton (TPLC), and (b) Rolleston (ROLC).

basin-generated surface waves (with periods of approximately $T = 6$ s), which are strongest in the fault normal component, consistent with the strongest SH waves in this component, but also evident in the fault-parallel and vertical-component velocity time series. In contrast, the effects of surface waves are relatively small at ROLC in Figure 4b.

NONLINEAR RESPONSE OF NEAR-SURFACE SOIL DEPOSITS

Another significant contribution to observed long-period ground motion amplitudes is the additional frequency-dependent amplification from nonlinear soil behavior, especially in the February 2011 event (Bradley and Cubrinovski 2011, Kaiser et al. 2012). A self-evident illustration of the significance of nonlinear soil response is possible from a comparison of two ground motions recorded at Lyttelton Port during the 22 February 2011 earthquake (Bradley and Cubrinovski 2011). One of the obtained motions is located on "engineering bedrock" (LPCC), while the other is located on a relatively thin (~30 m) colluvial layer (Bradley and Cubrinovski 2011). Figures 5a and 5b illustrate the acceleration

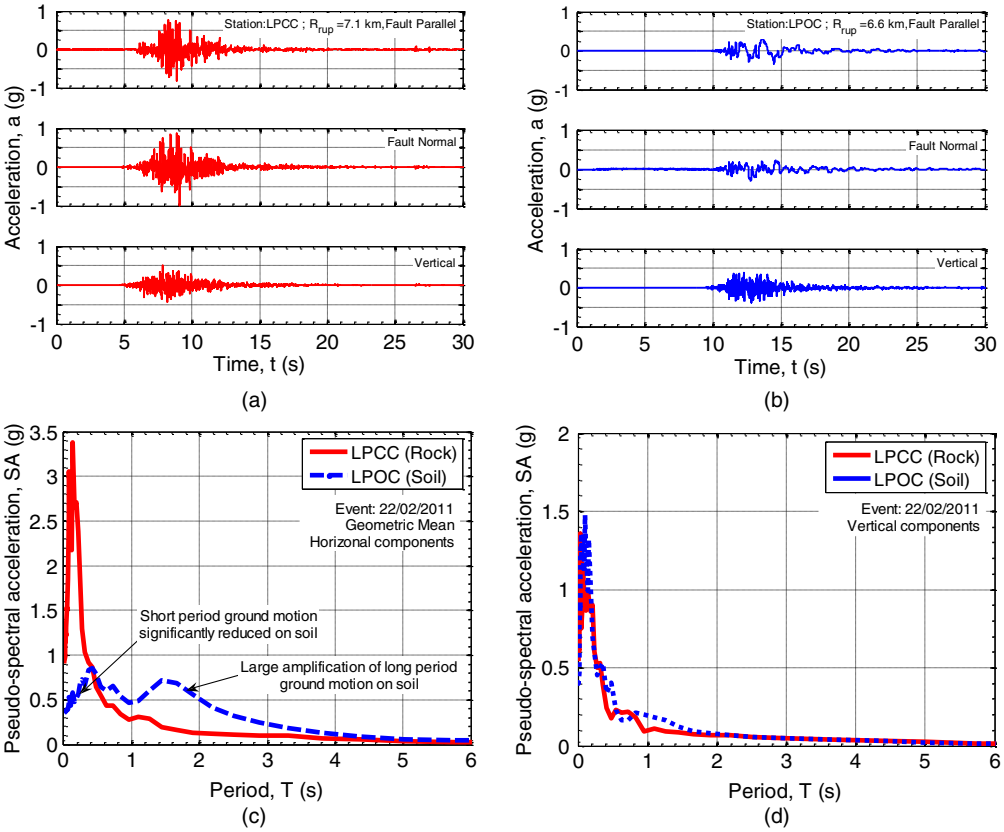

Figure 5. (a) and (b): Comparison of the acceleration time series recorded at Lyttelton Port during the 22 February 2011 earthquake at LPCC (rock) and LPOC (soil), respectively; (c) and (d): geometric mean horizontal and vertical component response spectra, respectively.

time series in three components at each of these two locations. The horizontal components of ground motion at the soil site have significantly lower amplitude, but are of longer periods, than those at the rock site. In contrast, the vertical accelerations at the two locations are similar. Figures 5c and 5d illustrate the pseudo-acceleration response spectra of the geometric mean horizontal and vertical ground motion components at the two sites. The observed horizontal ground motion at the LPOC site has significantly lower short-period ground motion amplitude, but notably larger response spectral amplitudes at longer periods. The vertical response spectra are very similar, as is evident from comparison of their time series.

COMPARISON WITH EMPIRICAL GROUND MOTION PREDICTION EQUATIONS

Figure 6 illustrates the pseudo-acceleration response spectra (SA) amplitudes of ground motions at periods of $T = 0.0$, 0.2, 1.0, and 3.0 s recorded within 50 km of the

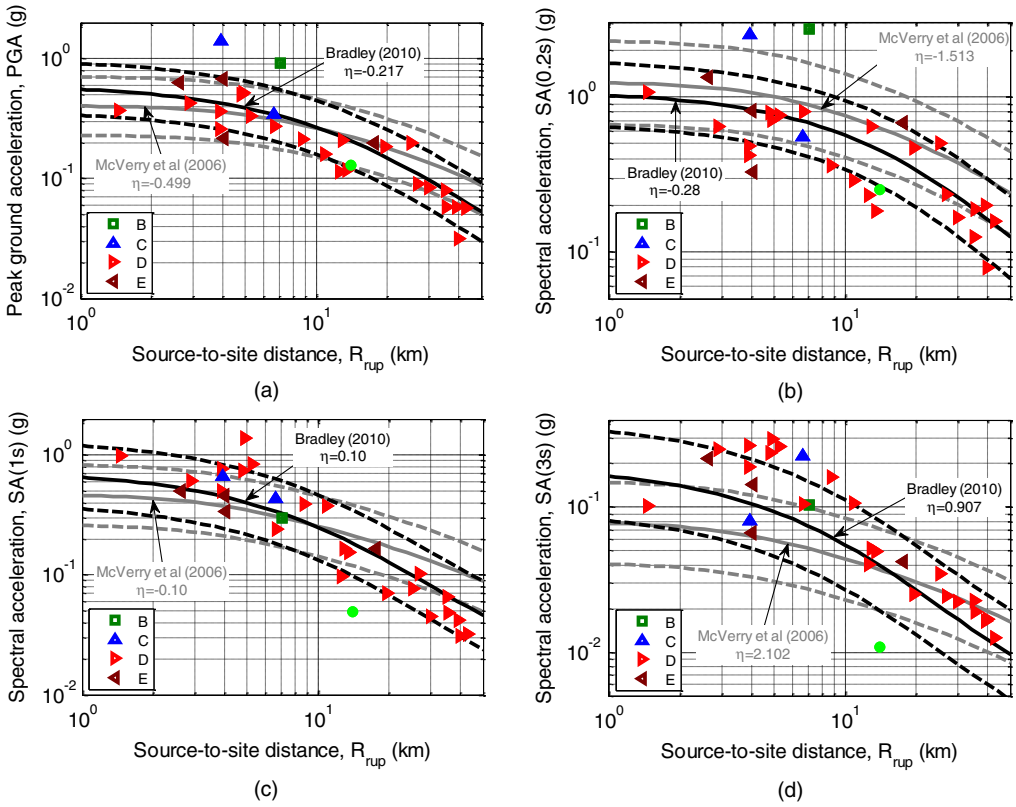

Figure 6. Comparison of pseudo-acceleration response spectral amplitudes observed in the 22 February 2011 Christchurch earthquake with empirical prediction equations of Bradley (2010, 2013) and McVerry et al. (2006) (site class D soil conditions): (a) PGA; (b) SA (0.2 s); (c) SA (1 s); and (d) SA (3 s). For each model, the median prediction is given by the solid line and 16th and 84th percentiles by dashed lines.

22 February 2011 Christchurch earthquake, in comparison with the median, 16th, and 84th percentiles of the empirical ground motion prediction equation of Bradley (2010, 2013) and McVerry et al. (2006; both models were developed prior to the Canterbury sequence). Figure 6 illustrates that the Bradley (2010) GMPE is able to capture the source-to-site distance dependence of the observations with good accuracy. In contrast, the McVerry et al. (2006) model is seen to have a weak scaling with source-to-site distance, often underpredicting near-source ground motions and overpredicting motions at moderate ($R_{rup} \geq 30$ km) source-to-site distances. The McVerry et al. model is also notably seen to systematically overpredict SA (0.2 s) amplitudes and underpredict SA (3.0 s) amplitudes. Further comparisons of these models with observations in the Canterbury sequence are given in Bradley (2012b).

CONCLUSIONS

This paper has provided a brief overview of the seismic source and ground motion aspects of the Canterbury earthquake sequence. The sequence includes four events over M_w5.9 that caused substantial damage to Christchurch city and its surroundings. These major events have well-documented complex rupture patterns with relatively large reported rupture displacements per unit fault length and stress drops. Surface rupture during the 4 September 2010 Darfield earthquake produced an approximately 30 km surface rupture in the Canterbury Plains with dextral surface displacements of several meters and a subordinate amount of vertical displacement, impacting residential structures, agricultural land, and river channels.

Dense recordings of ground motions in the near-source region of the major earthquake events illustrate significant effects of rupture directivity, basin-induced surface waves, and nonlinear local site effects. At short and moderate vibration periods, response spectral amplitudes predicted by the Bradley (2010) GMPE are consistent with observations, while at long vibration periods ($T > 3$ s) underpredictions generally occur, inferred as a result of forward directivity, basin-generated surface waves, and nonlinear surficial soil response. In the Central Business District, commercial structures were subjected to ground motions in the 22 February 2011 Christchurch earthquake well above the design levels for typical construction, while the amplitudes in the Darfield earthquake were approximately equal to design levels.

ACKNOWLEDGEMENTS

The paper benefited from constructive comments for three reviewers and the handling editor. Ground motion data were obtained from GeoNet (www.geonet.org.nz). Financial support from the New Zealand Earthquake Commission (EQC) is greatly appreciated.

REFERENCES

Beavan, J., Fielding, E., Motagh, M., Samsonov, S., and Donnelly, N., 2011. Fault location and slip distribution of the 22 February 2011 M_w 6.2 Christchurch, New Zealand, earthquake from geodetic data, *Seismological Research Letters* **82**, 789–799.

Beavan, J., Motagh, M., Fielding, E. J., Donnelly, N., and Collett, D., 2012. Fault slip models of the 2010–2011 Canterbury, New Zealand, earthquakes from geodetic data and observations of postseismic ground deformation, *New Zealand Journal of Geology and Geophysics* **55**, 207–221.

Beavan, J., Samsonov, S., Motagh, M., Wallace, L., Ellis, S., and Palmer, N., 2010. The Darfield (Canterbury) Earthquake: Geodetic observations and preliminary source model, *Bulletin of the New Zealand Society for Earthquake Engineering* **43**, 228–235, available at http://www.nzsee.org.nz/db/Bulletin/Archive/43(4)0228.pdf.

Bradley, B. A., 2010. *NZ-Specific Pseudo-Spectral Acceleration Ground Motion Prediction Equations Based on Foreign Models*, Department of Civil and Natural Resources Engineering, University of Canterbury, UC Research Report 2010-03, Christchurch, New Zealand, 324 pp, available at http://ir.canterbury.ac.nz/handle/10092/5126.

Bradley, B. A., 2012a. A critical analysis of strong ground motions observed in the 4 September 2010 Darfield earthquake, *Soil Dynamics and Earthquake Engineering*.

Bradley, B. A., 2012b. *Ground Motion and Seismicity Aspects of the 4 September 2010 and 22 February 2011 Christchurch Earthquakes*, Technical Report Prepared for the Canterbury Earthquakes Royal Commission, 62 pp, available at http://canterbury.royalcommission.govt.nz/documents-by-key/20120116.2087.

Bradley, B. A., 2012c. Strong ground motion characteristics observed in the 4 September 2010 Darfield, New Zealand earthquake, *Soil Dynamics and Earthquake Engineering* **42**, 32–46.

Bradley, B. A., 2013. A New Zealand-specific pseudo-spectral acceleration ground-motion prediction equation for active shallow crustal earthquakes based on foreign models, *Bulletin of the Seismological Society of America* **103**.

Bradley, B. A., and Cubrinovski, M., 2011. Near-source strong ground motions observed in the 22 February 2011 Christchurch earthquake, *Seismological Research Letters* **82**, 853–865.

Bray, J. D., and Kelson, K. I., 2006. Observations of surface fault rupture from the 1906 earthquake in the context of current practice, *Earthquake Spectra* **22**, S69–S89.

Brown, L. J., and Weeber, J. H., 1992. *Geology of the Christchurch Urban Area*, Geological and Nuclear Sciences, 110 pp.

Buchanan, A., Carradine, D., Beattie, G. J., and Morris, H., 2011. Performance of houses during the Christchurch earthquake of 22 February 2011, *Bulletin of the New Zealand Society for Earthquake Engineering* **44**, 342–357, available at http://www.nzsee.org.nz/db/Bulletin/Archive/44(4)0342.pdf.

Clifton, C., Bruneau, M., MacRae, G. A., Leon, R. T., and Fussell, A., 2011. Steel Structures Damage from the Christchurch earthquake series of 2010 and 2011, *Bulletin of the New Zealand Society for Earthquake Engineering* **44**, 297–318, available at http://www.nzsee.org.nz/db/Bulletin/Archive/44(4)0297.pdf.

Cubrinovski, M., Cubrinovski, M., Bradley, B., Wotherspoon, L., Green, R., Bray, J., Wood, C., Pender, M., Allen, J., Bradshaw, A., Rix, G., Taylor, M., Robinson, K., Henderson, D., Giorgini, S., Ma, K., Winkley, A., Zupan, J., O'Rourke, T., DePascale, G., and Wells, D., 2011a. Geotechnical Aspects of the 22 February 2011 Christchurch Earthquake, *Bulletin of the New Zealand Society for Earthquake Engineering* **44**, 205–226, available at http://www.nzsee.org.nz/db/Bulletin/Archive/44(4)0205.pdf.

Cubrinovski, M., Bray, J. D., Taylor, M., Giorgini, S., Bradley, B., Wotherspoon, L., and Zupan, J., 2011b. Soil liquefaction effects in the Central Business District during the February 2011 Christchurch earthquake, *Seismological Research Letters* **82**, 893–904.

Cubrinovski, M., Green, R. A., Allen, J., Ashford, S., Bowman, E., Bradley, B., Cox, B., Hutchinson, T., Kavazanjian, E., Orense, R., Pender, M., Quigley, M., and Wotherspoon, L., 2010. Geotechnical reconnaissance of the 2010 Darfield (Canterbury) earthquake, *Bulletin of the New Zealand Society for Earthquake Engineering* **43**, 243–320, available at http://www.nzsee.org.nz/db/Bulletin/Archive/43(4)0243.pdf.

Dellow, G. D., Yetton, M., Archibald, G., Barrell, D. J. A., Bell, D., Bruce, Z., Campbell, A., Davies, T., De Pascale, G., Easton, M., Forsyth, P. J., Gibbons, C., Glassey, P., Grant, H., Green, R., Hancox, G., Jongens, R., Kingsbury, P., Kupec, J., MacFarlane, D., McDowell, B., McKelvey, B., McCahon, I., McPherson, I., Molloy, J., Muirson, J., O'Halloran, M., Perrin, N., Price, C., Read, S., Traylen, N., Van Dissen, R., Villeneuve, M., and Walsh, I., 2011. Landslides caused by the 22 February 2011 Christchurch earthquake and management of landslide risk in the immediate aftermath, *Bulletin of the New Zealand Society for Earthquake Engineering* **44**, 227–238, available at http://www.nzsee.org.nz/db/Bulletin/Archive/44(4)0227.pdf.

Dizhur, D., Ismail, N., Knox, C., Lumantarna, R., and Ingham, J. M., 2010. Performance of unreinforced and retrofitted masonry buildings during the 2010 Darfield earthquake, *Bulletin of the New Zealand Society for Earthquake Engineering* **43**, 321–339, available at http://www.nzsee.org.nz/db/Bulletin/Archive/43(4)0321.pdf.

Duffy, B., Quigley, M., Barrell, D. J. A., Van Dissen, R., Stahl, T., Leprince, S., McInnes, C., and Bilderback, E., 2013. Fault kinematics and surface deformation across a releasing bend during the 2010 Mw 7.1 Darfield, New Zealand, earthquake revealed by differential LiDAR and cadastral surveying, *Geological Society of America Bulletin* **125**, 420–431.

Elliott, J. R., Elliott, J. R., Nissen, E. K., England, P. C., Jackson, J. A., Lamb, S., Li, Z., Oehlers, M., and Parsons, B., 2012. Slip in the 2010–2011 Canterbury earthquakes, New Zealand, *J. Geophys. Res.* **117**, B03401.

Fry, B., and Gerstenberger, M. C., 2011. Large Apparent Stresses from the Canterbury Earthquakes of 2010 and 2011, *Seismological Research Letters* **82**, 833–838.

Gledhill, K., Ristau, J., Reyners, M., Fry, B., and Holden, C., 2011. The Darfield (Canterbury, New Zealand) Mw 7.1 earthquake of September 2010: A preliminary seismological report, *Seismological Research Letters* **82**, 378–386.

Jongens, R., Barrell, D. J. A., Campbell, J. K., and Pettinga, J. R., 2012. Faulting and folding beneath the Canterbury Plains identified prior to the 2010 emergence of the Greendale Fault, *New Zealand Journal of Geology and Geophysics* **55**, 169–176.

Kaiser, A., Holden, C., Beavan, J., Beetham, D., Benites, R., Celentano, A., Collett, D., Cousins, J., Cubrinovski, M., Dellow, G., Denys, P., Fielding, E., Fry, B., Gerstenberger, M., Langridge, R., Massey, C., Motagh, M., Pondard, N., McVerry, G., Ristaua, J., Stirling, M., Thomas, J., Umaa, S. R., and Zhaoa, J., 2012. The Mw 6.2 Christchurch earthquake of February 2011: preliminary report, *New Zealand Journal of Geology and Geophysics* **55**, 67–90.

Kam, W. Y., Pampanin, S., and Elwood, K. J., 2011. Seismic performance of reinforced concrete buildings in the 22 February Christchurch (Lyttelton) earthquake, *Bulletin of the New Zealand Society for Earthquake Engineering* **44**, 239–278, available at http://www.nzsee.org.nz/db/Bulletin/Archive/44(4)0239.pdf.

Kerr, J., Nathan, S., Van Dissen, R., Webb, P., Brunsdon, D., and King, A., 2003. Planning for development of land on or close to active faults: a guideline to assist resource management planners in New Zealand, Ministry for the Environment, ME number 565, 67 pp.

NZS 1170.5, 2004. Structural Design Actions, Part 5: Earthquake Actions - New Zealand, Standards New Zealand, Wellington, New Zealand, p. 82.

Price, E. J., and Bürgmann, R., 2002. Interactions between the Landers and Hector Mine, California, earthquakes from space geodesy, boundary element modeling, and time-dependent friction, *Bulletin of the Seismological Society of America* **92**, 1450–1469.

Quigley, M., Van Dissen, R., Litchfield, N., Villamor, P., Duffy, B., Barrell, D., Furlong, K., Stahl, T., Bilderback, E., and Noble, D., 2012. Surface rupture during the 2010 Mw 7.1 Darfield (Canterbury) earthquake: Implications for fault rupture dynamics and seismic-hazard analysis, *Geology* **40**, 55–58.

Quigley, M. C., Bastin, S., and Bradley, B. A., 2013. Recurrent liquefaction in Christchurch, New Zealand, during the Canterbury earthquake sequence, *Geology* **41**, 419–422.

Rockwell, T. K., Lindvall, S. C., Dawson, T. E., Langridge, R. M., Lettis, W. R., and Klinger, Y., 2002. Lateral offsets on surveyed cultural features resulting from the 1999 Izmit and Duzce earthquakes, Turkey, *Bulletin of the Seismological Society of America* **92**, 79–94.

Van Dissen, R., Barrell, D., Litchfield, N., Villamor, P., Quigley, M., King, A., Furlong, K., Begg, J., Townsend, D., Mackenzie, H., Stahl, T., Noble, D., Duffy, B., Bilderback, E., Claridge, J., Klahn, A., Jongens, R., Cox, S., Langridge, R., Ries, W., Dhakal, R., Smith, A., Horblow, S., Nicol, R., Pedley, K., Henham, H., Hunter, R., Zajac, A., and Mote, T., 2011. Surface rupture displacement on the Greendale Fault during the Mw 7.1 Darfield (Canterbury) earthquake, New Zealand, and its impact on man-made structures, in *9th Pacific Conference on Earthquake Engineering*, Auckland, New Zealand, p. 8.

Van Dissen, R., Heron, D., Becker, J., King, A., and Kerr, J., 2006. Mitigating active fault surface rupture hazard in New Zealand: development of national guidelines, and assessment of their implementation, in *8th U.S. National Conference on Earthquake Engineering*, San Francisco, CA, p. 10.

Villamor, P., Litchfield, N., Barrell, D., Van Dissen, R., Hornblow, S., Quigley, M., Levick, S., Ries, W., Duffy, B., Begg, J., Townsend, D., Stahl, T., Bilderback, E., Noble, D., Furlongd, K., and Grante, H., 2012. Map of the 2010 Greendale Fault surface rupture, Canterbury, New Zealand: application to land use planning, *New Zealand Journal of Geology and Geophysics* **55**, 223–230.

Wallace, L. M., Beavan, J., McCaffrey, R., Berryman, K., and Denys, P., 2007. Balancing the plate motion budget in the South Island, New Zealand, using GPS, geological and seismological data, *Geophysical Journal International* **168**, 332–352.

(Received 1 March 2013; accepted 27 August 2013)